

A NUMERICAL APPROACH TO PREDICT THE ROTATING STALL IN THE VANELESS DIFFUSER OF A CENTRIFUGAL COMPRESSOR USING THE EIGENVALUE METHOD

CHENXING HU, PENGYIN LIU, XIAOCHENG ZHU

Co-Innovation Center for Advanced Aero-Engine, Shanghai Jiao Tong University, Shanghai, China
e-mail: ryanhu@sjtu.edu.cn; pengyinliu@163.com; zhxc@sjtu.edu.cn

HUA CHEN

National Laboratory of Engine Turbocharging Technology, Tianjin, China
e-mail: huachen204887@163.com

ZHAOHUI DU

Co-Innovation Center for Advanced Aero-Engine, Shanghai Jiao Tong University, Shanghai, China
e-mail: zhdu@sjtu.edu.cn

A two-dimensional incompressible flow model is presented to study the occurrence of rotating stall in vaneless diffusers of centrifugal compressors. The diffuser considered has two parallel walls, and the undisturbed flow is assumed to be circumferentially uniform, isentropic, and to have no axial velocity. The linearized 2D Euler equations for an incompressible flow in a fixed frame of the coordinate system are considered. After discretization by a spectral collocation method based on Chebyshev-Gauss-Lobatto points, the generalized eigenvalue problem is solved through the QZ algorithm. The compressor stability is judged by the imaginary part of the eigenvalue obtained. Based on the 2D stability analysis, the influence of inflow angle, radius ratio and wave number are studied. The results from the present stability analysis are compared with some experimental measurement and Shen's model. It is showed that diffuser instability increases rapidly and the stall rotational speed decreases quickly with an increase in the diffuser radius ratio. The largest critical inflow angle can be obtained when the wave number is around 3 ~ 5 for the radius ratio between 1.5 to 2.2. It is also verified that the stability model proposed in this paper agrees well with experimental data and has the capability to predict the onset of rotating stall, especially for wide diffusers.

Keywords: instability, vaneless diffuser, eigenvalue problem, spectral method

1. Introduction

Rotating stall in radial vaneless diffuser is one of the most common flow instabilities in centrifugal compressors and it can significantly influence the performance of the compressors. The nature of flow instability, especially rotating stall associated with vaneless diffusers have been extensively investigated by numerous researchers (Day, 2016; Everitt and Spakovszky, 2013; Spakovszky and Roduner, 2009; Ubben and Niehuis, 2015).

For decades, efforts have been made by researchers to explain the mechanism and predict the occurrence of rotating stall within the vaneless diffuser. Quantities of theoretical methodologies based on different assumptions and simplifications on the base flow have been proposed during that time. Generally speaking, one of the basic distinctions between the theoretical models on vaneless diffusers is whether the influence of the boundary layer is taken into consideration. The first type of approaches which was adopted by Jansen (1964), Senoo and Kinoshita (1977) and Frigne and Braembussche (1985) is that the three-dimensional wall boundary layer

is supposed to be responsible for the occurrence of rotating stall in a narrow vaneless diffuser. According to the experimental and theoretical study of Jansen (1964), the flow was assumed to be symmetric with respect to the diffuser depth and the local inward radial velocity component was treated as the inception of rotating stall. While in Senoo's vaneless diffuser model, the flow was no longer assumed to be symmetric and a non-uniform distribution of inlet velocity along the axial direction was taken into account. In his calculations, the critical velocity angle was defined for which reverse flow started in the vaneless diffuser (Senoo and Kinoshita, 1978).

On the other hand, an other theory for the occurrence of rotating stall in a vaneless diffuser, which was employed by Abdelhamid (1980) and Moore (1989), indicates that the stall is associated with two-dimensional core flow instability in vaneless diffusers which usually have the width radius ratio above 0.1. The two-dimensional numerical model developed by Moore is based on calculation of 2D incompressible Euler's equations. Neutrally stable rotating disturbances with low speed were found and a dense set of resonant solutions in which large pressure perturbations were taken as the criterion of rotating stall in Moore's work. Chen *et al.* (2011) extended the 2 dimensional model of Moore into a 3 dimensional model with consideration of the distribution of inlet velocity along the axial direction. Sun *et al.* (2013, 2016) proposed stability models for axial and centrifugal compressors on the basis of the eigenvalue approach. The comparisons with the results from experiments validated the effectiveness and accuracy of their models.

In addition, the significant influence of diffuser geometry and flow parameters on the vaneless diffuser performance and structure of the stall pattern have been also numerically and experimentally investigated in the recent years. The experiments carried out by Abdelhamid (1983) and Bianchini *et al.* (2013) confirmed that the local reverse flow did not necessarily lead to stall. The dependency of flow instability on the diffuser width ratios and diameter were also verified. The critical flow coefficient becomes larger with a decrease in diffuser width according to experiments of Abidogun (2002). Besides those experimental researches, the diffuser stability was also numerically investigated by Everitt (2010) through conducting isolated diffuser simulations, and the volute was found to have potential in delaying the onset of diffuser instability. Although the CFD method has an advantage over theoretical methods by providing a direct and vivid flow field with a relatively high accuracy, there is no a certain way for numerical simulation to capture the complicated disturbance with different frequency, amplitude and length scale due to unsteadiness and complexity of the flow field.

According to Jansen (1964), unsteady inviscid motion of the fluid is analyzed with the assumption that the disturbances can be expressed in terms of periodic waves. The equations are then reduced and solutions are sought for the resulting eigenvalue problem. However, it is mentioned in his paper that the prediction of the number of stall cells and the determination of the constant in the velocity equation requires a subsequent study.

In the present paper, firstly a 2D vaneless diffuser theoretical model based on stability analysis of an incompressible base flow is established and the full eigenvalue spectrum is obtained. Then the influence of collocation points and geometric parameters of the vaneless diffuser on the stability is investigated. Finally, the comparison between the results obtained from the present stability model and those from several experiments and models reported previously is performed. Compared to unsteady CFD simulations which are quite time and resources consuming and Senoo's stability model, which is unable to provide the stall number, the present analysis is able to predict the occurrence and stall number cheaply and quickly. And compared to Shen's model, the present model is easier to be extended to the stability problem concerning the sensitivity.

2. Theoretical model

2.1. Numerical methodology

In the present analysis, the stability discussed here is assessed by linearizing 2D Euler's equations for a base flow and determined by an operator that describes the evolution of small perturbations superposed on the base flow. The eigenvalues of this operator give the frequency and time growth rate of the perturbations. The corresponding eigenfunctions yield the mode shapes. The perturbation with the largest growth rate is the one that dominates the stability in the long term, and the positive growth rate means the occurrence of instability.

The diffuser considered has two parallel walls, and the undisturbed flow is assumed to be circumferentially uniform, isentropic, and to have no axial velocity. To further simplify the calculation, the perturbations and velocity distribution of the base flow along the axial direction are neglected. The flow sketch is shown in Fig. 1. The inflow circumferential angle α is defined at the diffuser inlet as illustrated in Fig. 1b. Then, a 2D flow model for study of the flow stability in the vaneless diffuser can be developed.

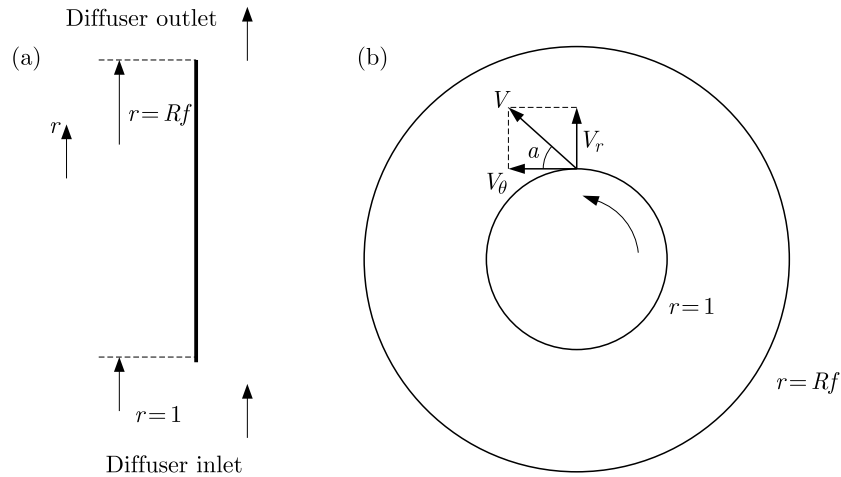


Fig. 1. Sketch of a vaneless diffuser: (a) base flow, (b) inflow angle

2.2. Implementation of the numerical model

2.2.1. Linearization of Euler's equations

To begin with, viscosity and compressibility are neglected in our study. The flow field is described by non-dimensionalized 2-D unsteady incompressible Euler's equations as shown

$$\begin{aligned}
 \frac{v_r}{r} + \frac{\partial v_r}{\partial r} + \frac{1}{r} \frac{\partial v_\theta}{\partial \theta} &= 0 \\
 \frac{\partial v_r}{\partial t} + v_r \frac{\partial v_r}{\partial r} + \frac{v_\theta}{r} \frac{\partial v_r}{\partial \theta} - \frac{v_\theta^2}{r} &= -\frac{\partial p}{\partial r} \\
 \frac{\partial v_\theta}{\partial t} + v_r \frac{\partial v_\theta}{\partial r} + \frac{v_\theta}{r} \frac{\partial v_\theta}{\partial \theta} + \frac{v_\theta v_r}{r} &= -\frac{\partial p}{r \partial \theta}
 \end{aligned} \tag{2.1}$$

Here, the velocity is non-dimensionalized by the impeller tip velocity U . The length is non-dimensionalized by the corresponding inlet radius r_1 and the time t is non-dimensionalized by r_1/U . Thus, v_r and v_θ mean the non-dimensionalized radial and circumferential velocities. In the stability analysis, the flow field is assumed to consist of the base flow and a small disturbance. Then, the velocity and pressure can be rewritten as follows

$$p = \bar{p} + p' \quad v_r = \bar{v}_r + v'_r \quad v_\theta = \bar{v}_\theta + v'_\theta \tag{2.2}$$

where \bar{p} represents base flow pressure and p' are small disturbances of pressure. For the base flow, V_r and V_θ represent the inlet radial and circumferential velocity of the base flow, respectively.

Before Eqs. (2.2) are substituted into Eqs. (2.1), emphasis on the small perturbation theory is made: 1) any disturbances of the 2nd and higher orders are neglected, 2) the base flow is treated as steady, so $\partial\bar{\bullet}/\partial t = 0$, c) since the mean flow is circumferentially symmetric, $\partial\bar{\bullet}/\partial\theta = 0$. And Eqs. (2.1) are still appropriate for the base flow. Then the linearized non-dimensional Euler's equations can be derived as follows

$$\begin{aligned} \frac{v'_r}{r} + \frac{\partial v'_r}{\partial r} + \frac{1}{r} \frac{v'_\theta}{\theta} &= 0 \\ \frac{\partial v'_r}{\partial t} + \frac{\partial \bar{v}_r}{\partial r v'_r} + \left(\bar{v}_\theta \frac{\partial v'_r}{r \partial \theta} + \bar{v}_r \frac{\partial v'_r}{\partial r} \right) - \frac{2\bar{v}_\theta v'_\theta}{r} + \frac{\partial p'}{\partial r} &= 0 \\ \frac{\partial v'_\theta}{\partial t} + v'_r \left(\frac{\partial \bar{v}_\theta}{\partial r} + \frac{\bar{v}_\theta}{r} \right) + \left(\bar{v}_\theta \frac{\partial v'_\theta}{r \partial \theta} + \bar{v}_r \frac{\partial v'_\theta}{\partial r} \right) + \frac{\bar{v}_r v'_\theta}{r} + \frac{\partial p'}{r \partial \theta} &= 0 \end{aligned} \quad (2.3)$$

2.2.2. Establishment of the eigenvalue problem

In general, the separation between spatial and temporal coordinates allows making use of Fourier modes in time when the variables are homogeneous. Then the perturbations can be written in form of $e^{i\theta}$ where the homogeneous variables (including time) are taken into account and the inhomogeneous variables are taken as the amplitude function. The specific form of the Fourier mode assumed is that the disturbances are normal modes in the circumferential direction, the disturbances can be written as follows

$$p' = P(r)e^{i(-\omega t + m\theta)} \quad v'_r = A(r)e^{i(-\omega t + m\theta)} \quad v'_\theta = W(r)e^{i(-\omega t + m\theta)} \quad (2.4)$$

where m is the azimuthal wavenumber and $\omega = \omega_r + i\omega_i$. Taking p' for instance as

$$p' = P(r)e^{im\theta} e^{(-i\omega_r + \omega_i)t} \quad (2.5)$$

it can be seen that corresponding to $e^{\omega_i t}$ dominates the growth rate of disturbances with time. Namely, if the imaginary part $\omega_i > 0$, the disturbances will grow exponentially with time, and the mode will be unstable. If $\omega_i < 0$, the disturbances will decay with time and the mode will be stable. And is the angular frequency.

The rotational speed of the disturbances in the circumferential direction non-dimensionalized by the impeller rotational speed is

$$f = \frac{-\omega_r}{m} \quad (2.6)$$

Substituting equations (2.4) into (2.3), the ordinary differential equations for A , W , P which represent $A(r)$, $W(r)$ and $P(r)$ with the subscript omitted, can be obtained as follows ($A'_r = dA/dr$ etc.)

$$\begin{aligned} A'_r + \frac{A}{r} + \frac{im}{r}W &= 0 \\ -i\omega A + \frac{\partial \bar{v}_r}{\partial r}A + \bar{v}_r A'_r + \frac{im\bar{v}_\theta A}{r} - \frac{2\bar{v}_\theta}{r}W + P'_r &= 0 \\ -i\omega W + A \left(\frac{\partial \bar{v}_\theta}{\partial r} + \frac{\bar{v}_\theta}{r} \right) + \bar{v}_r W'_r + \frac{im\bar{v}_\theta W}{r} + \frac{\bar{v}_r}{r}W + \frac{im}{r}P &= 0 \end{aligned} \quad (2.7)$$

Since there is no inlet disturbances coming from the outside of the system, homogeneous ordinary differential equations (2.7) can also expressed as

$$\mathbf{M}\phi = \omega \mathbf{J}\phi \quad (2.8)$$

where $\phi = [A, W, P]^T$, and \mathbf{M} and \mathbf{J} are the corresponding coefficient matrices

$$\mathbf{M} = \begin{bmatrix} \frac{1}{r} + \frac{\partial}{\partial r} & \frac{im}{r} & 0 \\ \frac{d\bar{v}_r}{dr} + \bar{v}_r \frac{\partial}{\partial r} + \frac{im\bar{v}_\theta}{r} & -\frac{r}{2\bar{v}_\theta} & \frac{\partial}{\partial r} \\ \frac{d\bar{v}_\theta}{dr} + \frac{\bar{v}_\theta}{r} & \bar{v}_r \frac{\partial}{\partial r} + \frac{im\bar{v}_\theta}{r} + \frac{\bar{v}_r}{r} & \frac{\partial}{\partial r} \end{bmatrix} \quad \mathbf{J} = \begin{bmatrix} 0 & 0 & 0 \\ i & 0 & 0 \\ 0 & i & 0 \end{bmatrix} \quad (2.9)$$

Solving equation (2.8) leads to a generalized eigenvalue problem, and the eigenvalue is used to determine the instability of the vaneless diffuser.

2.2.3. Establishment of the base flow

According to conservation of angular momentum and mass, the circumferential and radial velocity can be expressed as follows

$$\bar{v}_{r1} 2\pi r_1 = \bar{v}_r 2\pi r \quad \bar{v}_{\theta 1} r_1 = \bar{v}_\theta r \quad (2.10)$$

Therefore, the expressions of circumferential and radial velocity can be obtained as

$$\bar{v}_r = \frac{V_r}{r} \quad \bar{v}_\theta = \frac{V_\theta}{r} \quad (2.11)$$

where V_r and V_θ are the radial and circumferential velocity distributions at the diffuser inlet.

2.3. Discretization and calculation

2.3.1. Spatial discretization

Among the widely used spatial discretization methods, spectral methods have played a prominent role in early instability analyses. At present they are particularly useful. In this study, the spectral method is accomplished with Chebyshev-Gauss-Lobatto points. The two-dimensional linear eigenvalue problems posed above can be solved by constructing an operator that discretizes a n -th order linear ODE in the form of

$$L_{ij} = a_n(r_i) D_{ij}^{(n)} + \dots + a_1(r_i) D_{ij}^{(1)} + a_0(r_i) \quad (2.12)$$

where $D_{ij}^{(m)}$, $m = 1, 2, \dots, n$, is the m -th derivative matrix corresponding to the collocation points r_i , and a_0, a_1, \dots, a_n are evaluated at r_i .

When using spectral collocation methods, the value of the functions at collocation points is expressed as follows

$$\phi(r) = \sum_{j=0}^N \varphi_j(r) \tilde{\phi}(r_j) \quad (2.13)$$

where $\phi(r)$ is the value of the function at the point r obtained by using interpolant polynomials constructed for the variables in terms of their values at the collocation points, and $\varphi(r)$ is known as the basis function.

The collocation points in the calculation domain Ω are chosen as

$$r_\Omega = \cos \frac{\pi j}{N} \quad j = 0, 1, \dots, N \quad (2.14)$$

The extrema of the N -th order Chebyshev polynomial T_N are defined in the interval $-1 < r_\Omega < 1$. Then the interpolant $\varphi_j(r_\Omega)$ for the Chebyshev scheme is given as

$$\begin{aligned} \varphi_j(r_\Omega) &= \frac{1 - r_{\Omega j}^2}{r - r_{\Omega i}} \frac{T'_N(r_\Omega)}{N^2 c_j} (-1)^{j+1} \\ c_0 = c_N &= 2 \quad c_j = 1 \quad 0 < j < N \end{aligned} \quad (2.15)$$

The collocation derivative matrix \mathbf{D} for the Gauss-Lobatto grid is denoted by

$$D_{GL}^{(1)} = (d_{ij}) \quad 0 \leq i \quad j \leq N \quad (2.16)$$

where the elements d are defined by Canuto *et al.* (2010) as follows

$$d_{00} = -d_{NN} = \frac{2N^2 + 1}{6} \quad d_{jj} = \begin{cases} \frac{r_{\Omega j}}{2(r_{\Omega j}^2 - 1)} & 1 \leq j \leq N - 1 \\ \frac{c_i}{c_j} \frac{(-1)^{i+j}}{r_{\Omega i} - r_{\Omega j}} & i \neq j \end{cases} \quad (2.17)$$

In our case, the physical domain of interest $r \in [1, Rf]$ is mapped onto the standard collocation domain, based on the following equation

$$r_\Omega = -1 + 2 \frac{r - 1}{Rf - 1} \quad (2.18)$$

Thereby, linearized Euler's equation (2.8) can be illustrated in the collocation domain as follows

$$\mathbf{M}_\Omega \phi = \omega \mathbf{J}_\Omega \phi \quad (2.19)$$

For the 2D incompressible problem, when N collocation points are adopted to discretize the domain of interest, \mathbf{M}_Ω is a matrix of size $3N \times 3N$ arising from the three equations for the problem.

2.3.2. Numerical calculation of the generalized eigenvalue problem

One widely used algorithm for solving generalized eigenvalue problems is the QZ algorithm of Moler and Stewart (1973). This is a generalization of the QR algorithm for standard eigenvalue problems. Compared with other algorithms such as the Anorldi method (Meerbergen and Roose, 1997), inverse iteration (Peters and Wilkinson, 1979) and the Jacobi-Davidson method (Sleijpen and Van der Vorst, 1994), an important feature of the QZ algorithm is that it functions perfectly well with the presence of an infinite eigenvalue due to singularity of the matrix \mathbf{j}_Ω . In the current study, the calculation of the generalized eigenvalue problem proposed in equations (2.17) is carried out by the QZ algorithm. Matlab is a software with high capability on computational mathematics, and the function `eig` based on the QZ method in Matlab has been widely used for eigenvalue problems such as for the calculation in the present model. For a matrix with leading dimension of 200 in the present model, the calculation with the function `eig` can be quite time-saving.

What should be paid much attention to is that spurious eigenvalues derived from numerical calculation rather than real physical problem also exist while using the QZ algorithm. One way to distinguish the spurious eigenvalues from the real ones is to vary the number of collocation points. The eigenvalues which remain the same are the real ones.

3. Validation of the model

3.1. Influence of the collocation point number on the calculations

Firstly, the number of collocation points and its independence of the calculation is verified through changing this number. The eigenvalue spectra with different numbers of collocation points N at $Rf = 2$, $V_r = 0.1$, $m = 1$ are shown in Fig. 2.

It can be seen that although the largest eigenvalue with the same imaginary part can be obtained for all numbers of collocation points, the number larger than 50 is preferred to have a proper, whole sketch of the eigenvalue spectrum. In the subsequent study, 50 collocation points are adopted in the following calculations considering both numerical accuracy and computational efficiency. When the collocation number is more than 200 in the subsequent study, a 600×600 matrix is solved, and spurious eigenvalues which are at least two orders of magnitude higher than the real ones come into being.

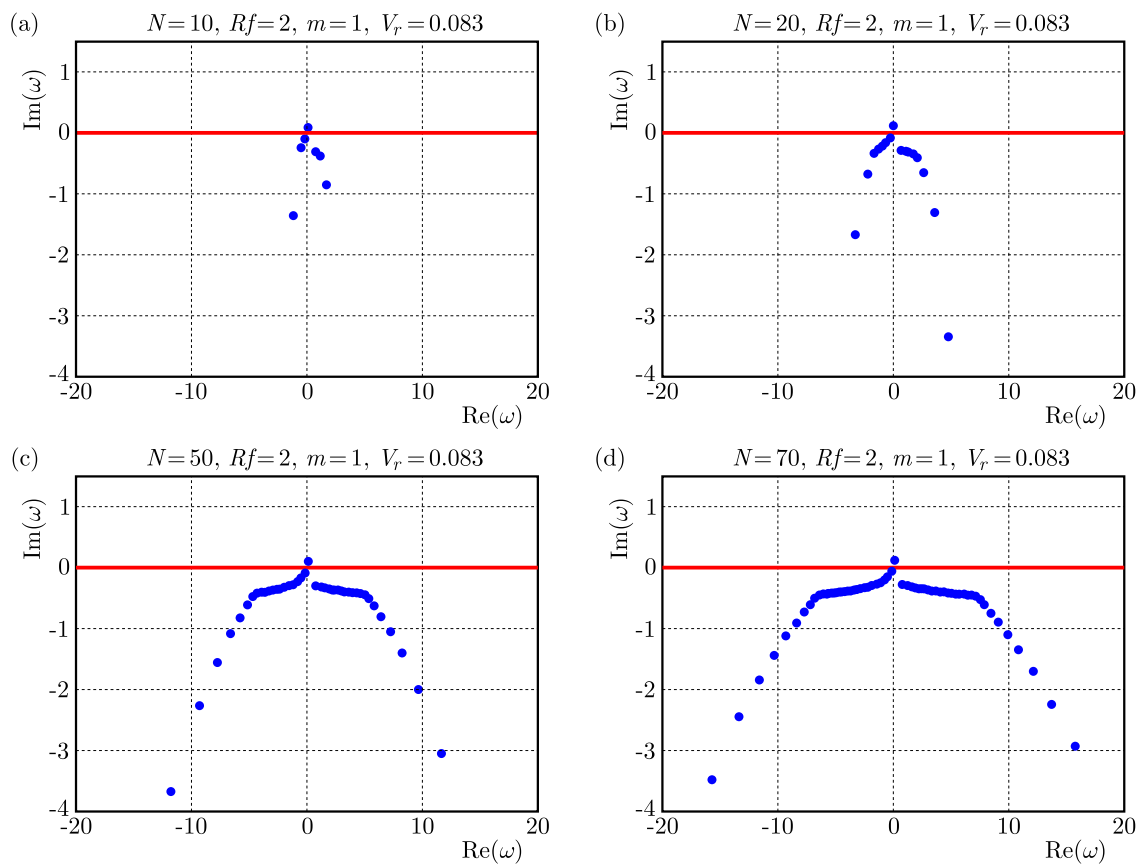


Fig. 2. Eigenvalue spectrum for different numbers of collocation points

3.2. Influence of diffuser inlet velocity of the base flow on the calculations

Generally, the inlet radial velocity distribution of the diffuser is highly influenced by the impeller, and the axial uniform radial velocity can seldom be obtained in a practical diffuser flow. However, the uniform distributed radial velocity for an inviscid flow is associated with the average inflow angle. A brief connection between the average inflow angle and diffuser stability can be revealed rapidly with the help of the present 2D stability model. Figure 3 shows the influence of variability of the inlet velocity of the base flow V_r on the stability of the vaneless diffuser with the same number N of collocation points, radius ratio Rf and wave number m . Different inflow angles are also listed corresponding to different inlet velocities.

It can be seen that with a decrease in the inlet radial velocity of the base flow, the flow in the vaneless diffuser turns from stability to instability. In other words, with a decrease in the inlet circumferential flow angle, the flow in the vaneless diffuser tends to instability, which well agrees with Senoo and Kinoshita (1978). Correspondingly, the inflow circumferential velocity angle when the rotating stall occurs is taken as the critical inflow angle α_c .

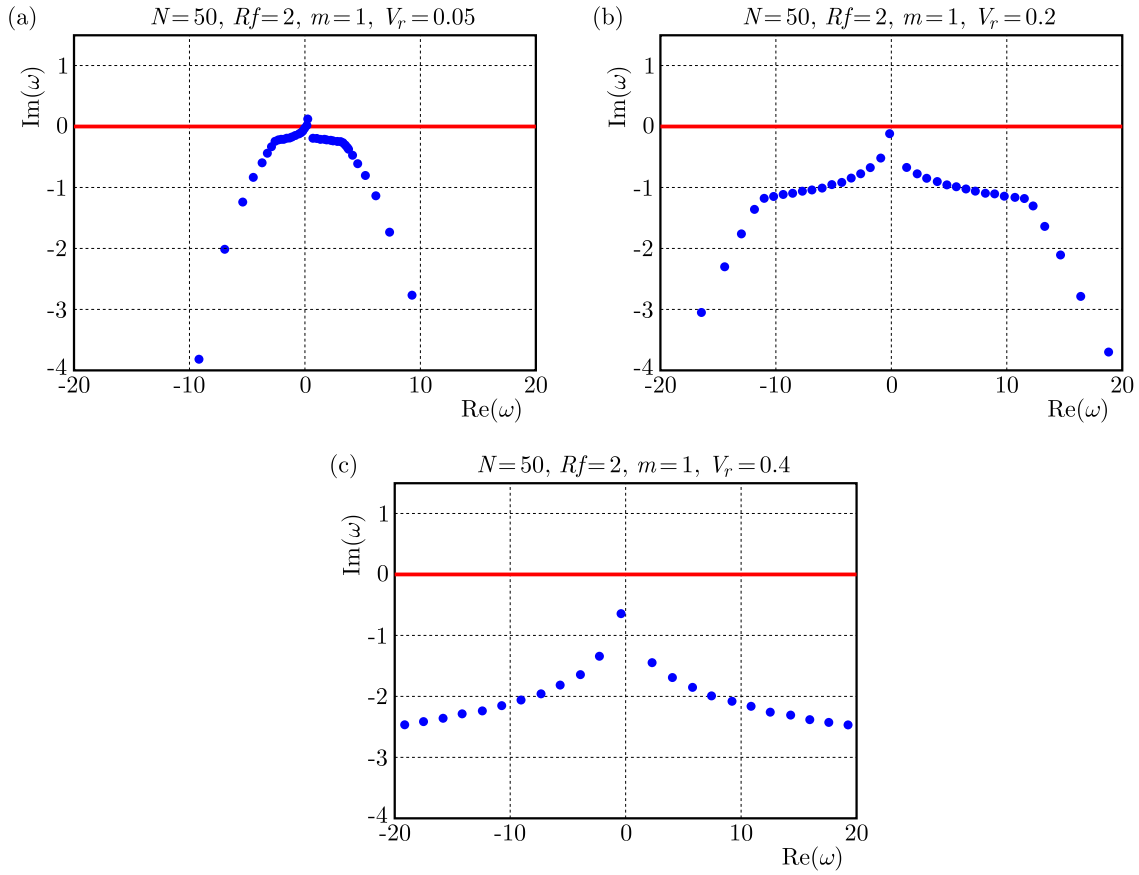


Fig. 3. Eigenvalue spectrum for different inlet radial velocities of the base flow

3.3. Influence of geometric parameters on the instability

3.3.1. Influence of the radius ratio Rf

As shown in Table 1, six leading eigenvalues in a descending order of the imaginary part of ω are presented. Compared with the cases for $Rf = 1.5$ and 1.67 , the imaginary part of the leading eigenvalue for $Rf = 2$ and 2.2 become positive. The leading eigenmode of the cases with larger values of Rf turns to instability. A larger value of the imaginary part of the leading eigenvalue indicates a higher time growth rate, which means stronger instability of the flow field. Therefore, the flow tends to instability with an increase in Rf .

3.3.2. Influence of the wave number m

A common feature of the centrifugal compression system is that it exhibits two kinds of rotating stall. One is known as the impeller stall, having a relatively high rotational speed of usually more than 50% of the impeller speed; and the other known as the diffuser stall, having a slower rotational speed at about 10% of the impeller speed. The present stability model is also applicable to confirmation of the stall number and rotational speed, therefore 3 cases with different radius ratios Rf are calculated for 5 different wave numbers m .

Table 1. Six leading eigenvalues for different values of Rf with $V_r = 0.131$, $N = 50$ and $m = 1$

$Rf = 1.5$	$Rf = 1.67$	$Rf = 2$	$Rf = 2.2$
$-0.10977 - 0.25458i$	$-0.024169 - 0.05096i$	$0.03898 + 0.079355i$	$0.05377 + 0.104624i$
$-2.91568 - 0.64371i$	$-2.22947 - 0.323566i$	$-2.01654 - 0.236903i$	$-0.29436 - 0.223245i$
$0.70504 - 0.72005i$	$0.332469 - 0.474960i$	$-2.87547 - 0.395488i$	$-1.7518 - 0.28062i$
$-4.28143 - 0.86662i$	$-3.180583 - 0.49452i$	$0.327611 - 0.416233i$	$-2.18808 - 0.32481i$
$2.04559 - 0.91810i$	$1.25444 - 0.59218i$	$-3.73096 - 0.495389i$	$-2.623871 - 0.33961i$
$-5.62630 - 1.01110i$	$-4.12054 - 0.60255i$	$1.161860 - 0.514977i$	$-0.08285 - 0.38274i$

When $m = 0$, the flow tends to be stable under any inlet flow condition. This is because that the time growth rate of circumferential disturbances are the main concern in our study, and zero wave number in the circumferential direction indicates that the circumferential disturbances are neglected, resulting in the absolutely stable condition in the calculation.

As shown in Fig. 4a, the influence of the wave number m on the critical stall angle is illustrated. It is clearly shown that the critical angle decreases with a decrease in Rf . According to Abidogum (2002), the most unstable mode (or stall) is often obtained for the wave number m of 3. It can be seen that the largest critical angle is obtained when m is around 3 with the radius ratio of 2.2. This is consistent with the result of Abidogum. The wave number corresponding to the most unstable mode differs for various radius ratios.

In Fig. 4b, the rotational speed of the disturbance corresponding to the onset of instability f vs. the wave number m is illustrated. It can be seen that the rotational speed of disturbance linearly increases with an increase in the wave number m while the wave speed decreases quickly with the diffuser radius ratio, which is consistent with the results of Moore (1989) and Chen *et al.* (2011).

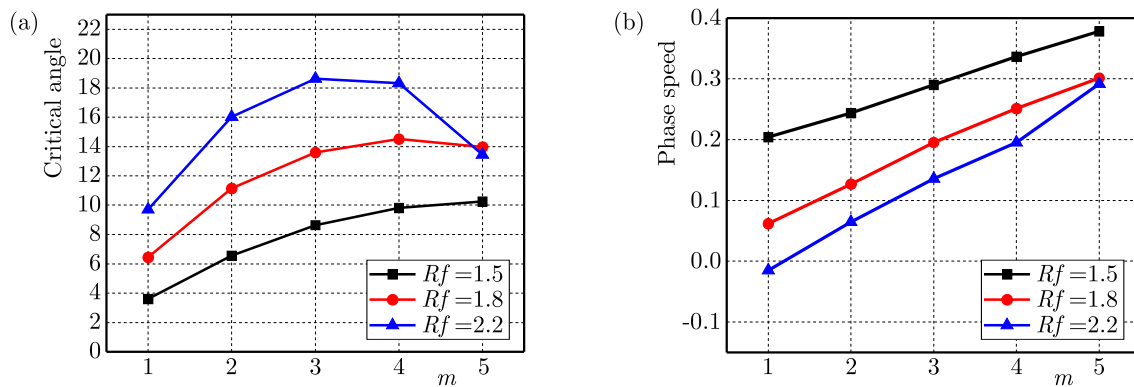


Fig. 4. Influence of the wave number m on the critical angle and rotational speed: (a) critical angle vs. wave number, (b) rotational speed vs. wave number

3.4. Some eigenfunctions

In the theory of linear stability, the maximum response to variable initial conditions are what we concern the most. In the present analysis, the amplification of disturbances is characterized in terms of the least stable mode of the matrix \mathbf{M} . The eigenvalue spectrum when the radius ratio Rf is 2, wave number m is 1 and the inlet radial velocity is 0.04 are shown in Fig. 5. Among the eigenvalues obtained, the leading three least stable eigenvalue spectra are selected and labeled as ω_1 , ω_2 , ω_3 . The eigenfunctions for pressure and velocity perturbations corresponding to the three different eigenvalues are illustrated in Fig. 6, respectively. The eigenfunctions corresponding to the three eigenvalues are proved to be sort of non-orthogonal. The non-normality of the linearized Euler equations has influence on the growth rate of the perturbations in a short timescale.

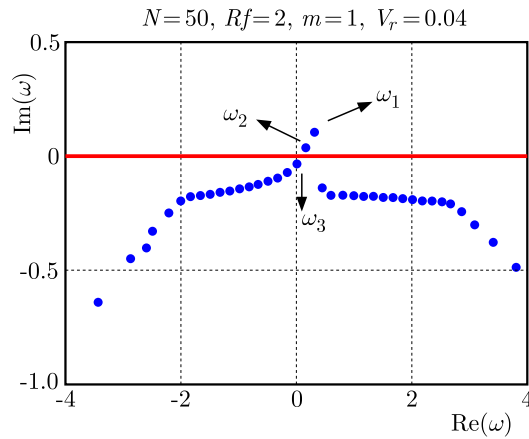


Fig. 5. Eigenvalue spectrum for $Rf = 2$, $m = 1$, $V_r = 0.04$

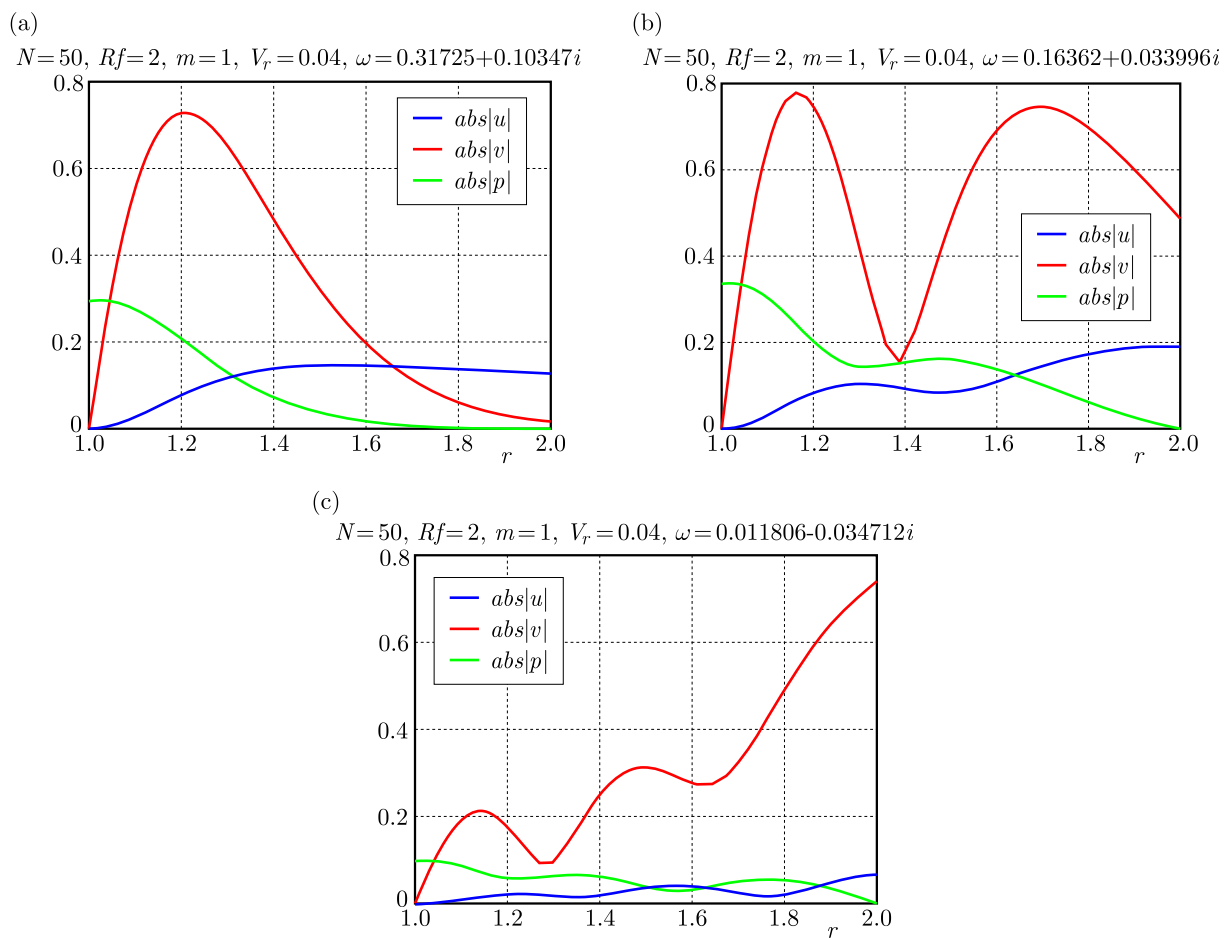


Fig. 6. Eigenfunctions corresponding to three eigenvalues for pressure and velocity perturbations: (a) ω_1 , (b) ω_2 , (c) ω_3

4. Application of the present stability model

4.1. Comparison with experimental results in (Kinoshita and Senoo, 1985)

In order to verify the results of the present analysis, the experiment results by Kinoshita and Senoo (1985) are compared with the predictions from the 2D stability model. In the experiment by Kinoshita and Senoo (1985), a back sweep angle of $\beta = 24.6^\circ$ was set at the impeller exit,

and two different values of the radial ratio Rf were tested. The experiment was undertaken at a low speed, and the inlet velocity distribution was not reported. The present 2D incompressible stability model has been applied to the experimental set up with a uniform inlet velocity distribution.

Since the rotating stall number observed in (Kinoshita and Senoo, 1985) is 3, the comparison of the critical flow angle in (Kinoshita and Senoo, 1985), Shen's in (Chen *et al.*, 2011) and the present method for the wave number $m = 3$ is given in Table 2. It can be shown that the result of the present stability analysis is much closer to the experiential data by Kinoshita and Senoo (1985) than those derived from Shen's 3D model.

Table 2. Comparison of the critical flow angle from experiment (Kinoshita and Senoo, 1985), Shen's result and current analysis

Rf	β [°]	m	α [°]		
			experiment	Shen	present model
1.4	24.6	3	5.2	7.925	6.657
1.67	24.6	3	5.5	12.82	11.631

At a smaller Rf , the agreement between the current method and the experiment is good. At the same time, this study suggests that the flow becomes significantly less stable for a larger radial ratio, whereas the experiment shows only a small deterioration of the stability.

4.2. Comparison with the experimental results in (Abidogun, 2002)

In (Abidogun, 2002) the experimental rig, as shown in Fig. 7, consists of an impeller with radial blades and a vaneless diffuser. Three different values of Rf were tested. According to the results given in (Abidogun, 2002), the stall wave number were always between 2-4. What makes rig in (Abidogun, 2002) different from that in (Kinoshita and Senoo, 1985) is the larger axial width b_z (> 0.1), which is more suitable for the models based on inviscid core flow theories such as Shen's and the present analysis.

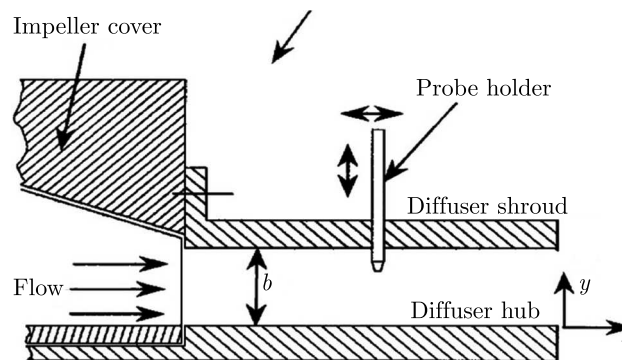


Fig. 7. The experimental rig for a vaneless diffuser in (Abidogun, 2002)

It is illustrated in Table 3 that the inlet critical flow velocity at the onset of stall derived by Abidogun (2002), Shen's model and the present stability analysis shows the same trend of increase with the diffuser radial ratio Rf . For a smaller radius ratio of the diffuser Rf , the prediction results of the present model and Shen's model show a higher accuracy than those for the radius ratio 2.0. Compared with the results in (Kinoshita and Senoo, 1985), the predicted critical inlet velocity for different radius ratios obtained in this test are all much closer to the experimental results. One main reason for this lies in that the present analysis and Shen's model are both based on the core flow assumption, which is more suitable for vaneless diffusers with large width.

Table 3. Comparison of the inlet critical flow in (Abidogun, 2002), Shen's and the present stability analysis

Rf	m	V_{rc}		
		Abidogun	Shen	present model
1.5	3	0.16	0.1525	0.152
1.7	3	0.216	0.2150	0.215
2.0	3	0.255	0.2925	0.294

5. Conclusions

In this research, a two dimensional stability model of a vaneless diffuser in a centrifugal compressor based on stability analysis is proposed. The independence of the number collocation points and the influence of geometric parameters on the stability of the vaneless diffuser are verified. The capability of the present model to predict the onset of stall with different radius ratios is validated against several experimental data. The present model is effective in stall prediction for a wide vaneless diffuser. Compared to Moore's and Shen's stability models, the advantage of the present model lies in direct calculation and providing both the complex eigenspectrum and rotational speed instead of multiple trials and iterations. Another remarking superiority is that the present model investigates the instability induced by the inviscid main flow, and provides the fundamental research for further study of the unsteady interaction of the inviscid main flow and the boundary layers.

In our investigation, the significant effects of the diffuser radius ratio on diffuser stability are confirmed. The stability deteriorates rapidly with an increase in the radius ratio. The largest critical inflow angle is obtained when the wave number m is around 3-5 for the radius ratio between 1.5 to 2.2. Through model assessment, this model has the capability of predicting the onset of stall in vaneless diffusers and can be applied in the cases without considering the axial distribution of inlet velocity. However, in the cases where the axial distribution of inlet velocity plays significant role, the application of a 3D stability model is required.

References

1. ABDELHAMID A.N., 1980, Analysis of rotating stall in vaneless diffusers of centrifugal compressors, *Canadian Aeronautics and Space Journal*, **26**, 118-128
2. ABDELHAMID A.N., 1983, Effects of vaneless diffuser geometry on flow instability in centrifugal compression systems, *Canadian Aeronautics and Space Journal*, **29**, 259-266
3. ABIDOGUN K.B., 2002, Effects of vaneless diffuser geometries on rotating stall, *Journal of Propulsion and Power*, **22**, 3, 542-549
4. BIANCHINI A., BILIOTTI D., BELARDINI E., GIACHI M., TAPINASSI L., VANNINI G., FERRARI L., FERRARA G., 2013, A systematic approach to estimate the impact of the aerodynamic force induced by rotating stall in a vaneless diffuser on the rotordynamic behavior of centrifugal compressor, *Journal of Engineering for Gas Turbines and Power*, **135**, 11
5. CANUTO B.C., HUSSAINI M.Y., QUARTERONI A., ZANG T.A., 2010, *Spectral Methods: Evolution to Complex Geometries and Applications to Fluid Dynamics*, Springer
6. CHEN H., SHEN F., ZHU X.C., DU Z.H., 2011, A 3D compressible flow model for weak rotating waves in vaneless diffusers. Part I: The model and Mach number effects, *Journal of Turbomachinery*, **134**, 4, 041010
7. DAY I.J., 2016, Stall, surge, and 75 years of research, *Journal of Turbomachinery*, **138**

8. EVERITT J.N., 2010, Investigation of stall inception in centrifugal compressors using isolated diffuser simulations, M.S. Thesis, MIT, Cambridge, MA
9. EVERITT J., SPAKOVSKY Z., 2013, An investigation of stall inception in centrifugal compressor vaneless diffuser, *Journal of Turbomachinery*, **135**
10. FRIGNE P., BRAEMBUSSCHE R.V.D., 1985, A theoretical model for rotating stall in the vaneless diffuser of a centrifugal compressor, *Journal of Engineer for Gas Turbines and Power*, **107**, 2, 507-513
11. JANSEN W., 1964, Rotating stall in a radial vaneless diffuser, *ASME Journal of Basic Engineering*, **86**, 4, 750-758
12. KINOSHITA Y., SENOO Y., 1985, Rotating stall induced in vaneless diffusers of very low specific speed centrifugal blowers, *Journal of Engineering for Gas Turbines and Power*, **107**, 514-521
13. MEERBERGEN K., ROOSE D., 1997, The restarted Arnoldi method applied to iterative linear system solvers for the computation of rightmost eigenvalues, *SIAM Journal on Matrix Analysis and Applications*, **18**, 1, 1-20
14. MOLER C.B., STEWART G.W., 1973, An algorithm for generalized matrix eigenvalue problems, *SIAM Journal on Numerical Analysis*, **10**, 2, 241-256
15. MOORE F.K., 1989, Weak Rotating flow disturbances in a centrifugal compressor with a vaneless diffuser, *Journal of Turbomachinery*, **111**, 442-449
16. PETERS G., WILKINSON J.H., 1979, Inverse iteration, Ill-conditioned equations and Newton's method, *SIAM Review*, **21**, 3, 339-360
17. SENOO Y., KINOSHITA Y., 1977, Influence of inlet flow condition and geometries of a centrifugal vaneless diffuser on critical flow angle for reverse flow, *Journal of Fluids Engineering*, **99**, 1, 98-103
18. SENOO Y., KINOSHITA Y., 1978, Limits of rotating stall and stall in vaneless diffuser of centrifugal compressors, *ASME Paper 78-GT-19*
19. SLEIJPEN G.L.G., VAN DER VORST H.A., 1994, A Jacobi-Davidson iteration method for linear eigenvalue problems, *SIAM Review*, **17**, 2, 267-293
20. SPAKOVSKY Z., RODUNER C., 2009, Spike and modal stall inception in an advanced turbocharger centrifugal compressor, *Journal of Turbomachinery*, **131**
21. SUN X.F., LIU X.H., SUN D.K., SUN X., 2013, A theoretical model for flow instability inception in transonic fan/compressors, *ASME Turbo Expo 2013: Turbine Technical Conference and Exposition*
22. SUN X.F., MA Y.F., LIU X.H., SUN D.K., 2016, Flow stability model of centrifugal compressor based on eigenvalue approach, *AIAA Journal*
23. UBBEN S., NIEHUIS R., 2015, Experimental investigation of the diffuser vane clearance effect in a centrifugal compressor stage with adjustable diffuser geometry. Part I: Compressor performance analysis, *Journal of Turbomachinery*, **137**